

An analytical approach on (U-Th)/He dating by sample encapsulation in quartz ampoules under vacuum: application to goethite, Amerasian Basin, Arctic Ocean

Olga Valentinovna Yakubovich^{1,2}, Natalia Pavlovna Konstantinova^{2,3}, Maria Olegovna Anosova⁴, Mary
5 Markovna Podolskaya⁵, Elena Valerevna Adamskaya²

¹Department of geochemistry, Saint-Petersburg University, St. Petersburg, 199034, Russia

²Laboratory of Isotope Geology, Institute of Precambrian Geology and Geochronology RAS, St. Petersburg, 199034, Russia

³Institute for Geology and Mineral Resources of the Ocean (VNIIOkeangeologia), St. Petersburg, 190121, Russia

⁴Vernadskiy institute of Geochemistry and Analytical Chemistry, Moscow, 119991, Russia

10 ⁵AnalyteMe, Reus, Tarragona, 43201, Spain

Correspondence to: Olga Yakubovich (olya.v.yakubovich@gmail.com)

Abstract

We propose a new analytical approach for (U-Th)/He dating of Fe-(oxyhydr)oxides, that includes sealing samples in quartz
15 ampoules and demonstrates its suitability as a reliable tool for the investigation of geological processes. The (U-Th)/He ages
of goethite clasts and vein from Fe- and Mn-oxide mineralization rocks recovered from the slope of Chukchi Borderland in
the Amerasia Basin demonstrate reproducibility, yielding a weighted mean age of 8.6 ± 0.3 Ma (n=4) and 4.8 ± 0.4 Ma (n=2),
respectively, providing insights into the Neogene mineralization history of the region. This study also focuses on the sample
preparation technique, that might influence the (U-Th)/He ages. Our data indicate that some of U can be leached from the
20 goethite during sonication by distilled water which might result in erroneous (U-Th)/He ages of multi-mineral grains.

1. Introduction

The (U-Th)/He dating method is based on the alpha-decay of U and Th that produce helium atoms. The accumulated ⁴He
component is used to determine the mineral age. Traditionally, the ⁴He isotopic systems have been successfully applied to low-
temperature thermochronology (Farley and Stockli, 2002). Recent developments in understanding how helium behaves in
25 various minerals have extended the method applicability in geochronological studies (Yakubovich et al. 2019; Shukolyukov
et al. 2012; Flowers et al. 2023 and references therein).

Fe-oxides and Fe-hydroxides, including goethite (α -FeO(OH)), lepidocrocite (γ -FeO(OH)), hematite (α -Fe₂O₃), maghemite (γ -Fe₂O₃) and magnetite (Fe²⁺Fe³⁺₂O₄), typically contain trace amounts of U and Th and therefore have been recognized as a potential geochronometer tool from the early days of geochronology (Strutt, 1908, 1909).

30 Goethite is one of the most common Fe- (oxy)hydroxide minerals formed during the hydrolyzation of rocks, making it a desirable mineral for dating various surface and subsurface geological processes. Helium diffusion studies revealed sufficient ⁴He retentivity in goethite in the range of the near-surface temperatures and make the mineral suitable for the (U-Th)/He weathering geochronology (Shuster et al., 2005).

The (U-Th)/He dating of goethite was applied successfully in dating of weathering profiles (e.g. Monteiro et al., 2014; Riffel et al., 2016; Ansart et al., 2022), supergene ore formation (e.g. Vasconcelos et al., 2013; Heller et al., 2022; Verhaert et al., 2022), and diagenetic transformations (Reiners, 2014). The approach was also implemented successfully in dating deep-sea hydrothermal Fe-oxide mineralization (Benites et al., 2022). However, the dating of hydrogenetic Fe-Mn crusts is not robust due to the significant content of extraterrestrial He-rich dust and their high porosity, that prevent the accumulation of radiogenic He (Basu et al., 2006).

40 The (U-Th)/He dating of surface processes is challenging due to the multistage Fe-hydroxides formation. Several generations of the same phase intimately intergrow in a millions years time span (Vasconcelos et al., 2013; Monteiro et al., 2014; Heller et al., 2022). Presence of small inclusions of U- and Th-bearing contaminants may add difficulties to the interpretation of the isotopic results. Thus, high-resolution mineralogical and paragenetic characterization of the sample is required which typically includes optical observations accompanied by XRD, SEM and chemical analyses (e.g. Monteiro et al., 2014; Hofmann et al., 2017; Deng et al., 2017).

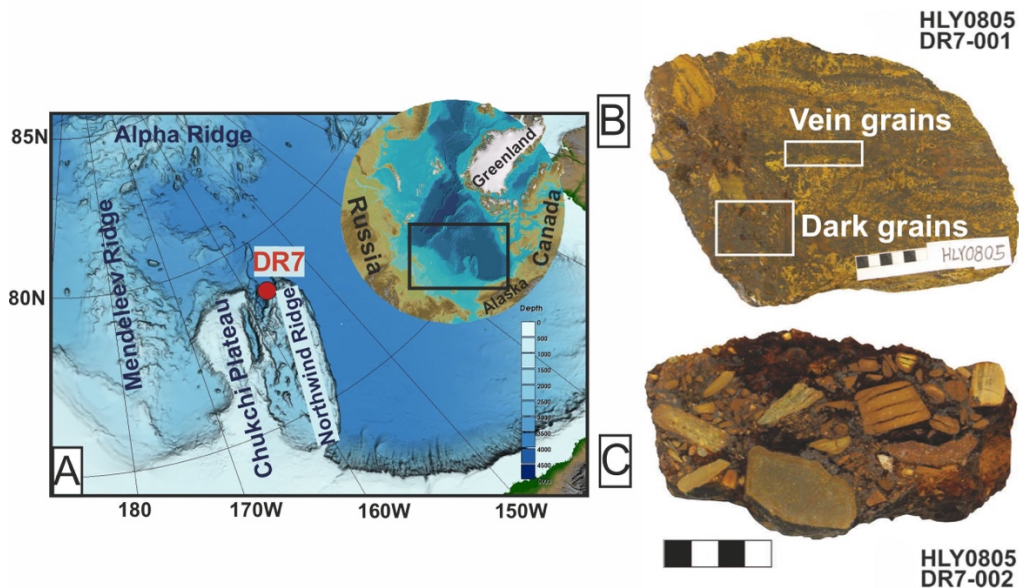
From the analytical point of view (U-Th)/He dating of goethite is challenging as well. The distribution of U and Th in the mineral is inhomogeneous (Shuster et al., 2005), therefore parental and daughter isotopes should be measured in the same sample. Helium release from the goethite must be carried out under strictly controlled laboratory heating conditions; otherwise, U and Th may be lost from the grains during He extraction rendering the results inaccurate (Vasconcelos et al., 2013). There are several approaches to overcome this issue such as heating in the presence of oxygen (Hofmann et al., 2020), using double-aliquot (Wernicke and Lippolt, 1993; Pidgeon et al., 2004), or multi-aliquot procedures (Wu et al., 2019). The last two require remarkably larger amount of material.

Here, we propose the alternative (U-Th)/He dating methodology using an example of goethite from the Chukchi Borderland, Arctic Ocean. The technique was originally developed for (U-Th)/He dating of native gold (Yakubovich et al. 2014) and pyrite (Yakubovich et al. 2020).

2. Samples

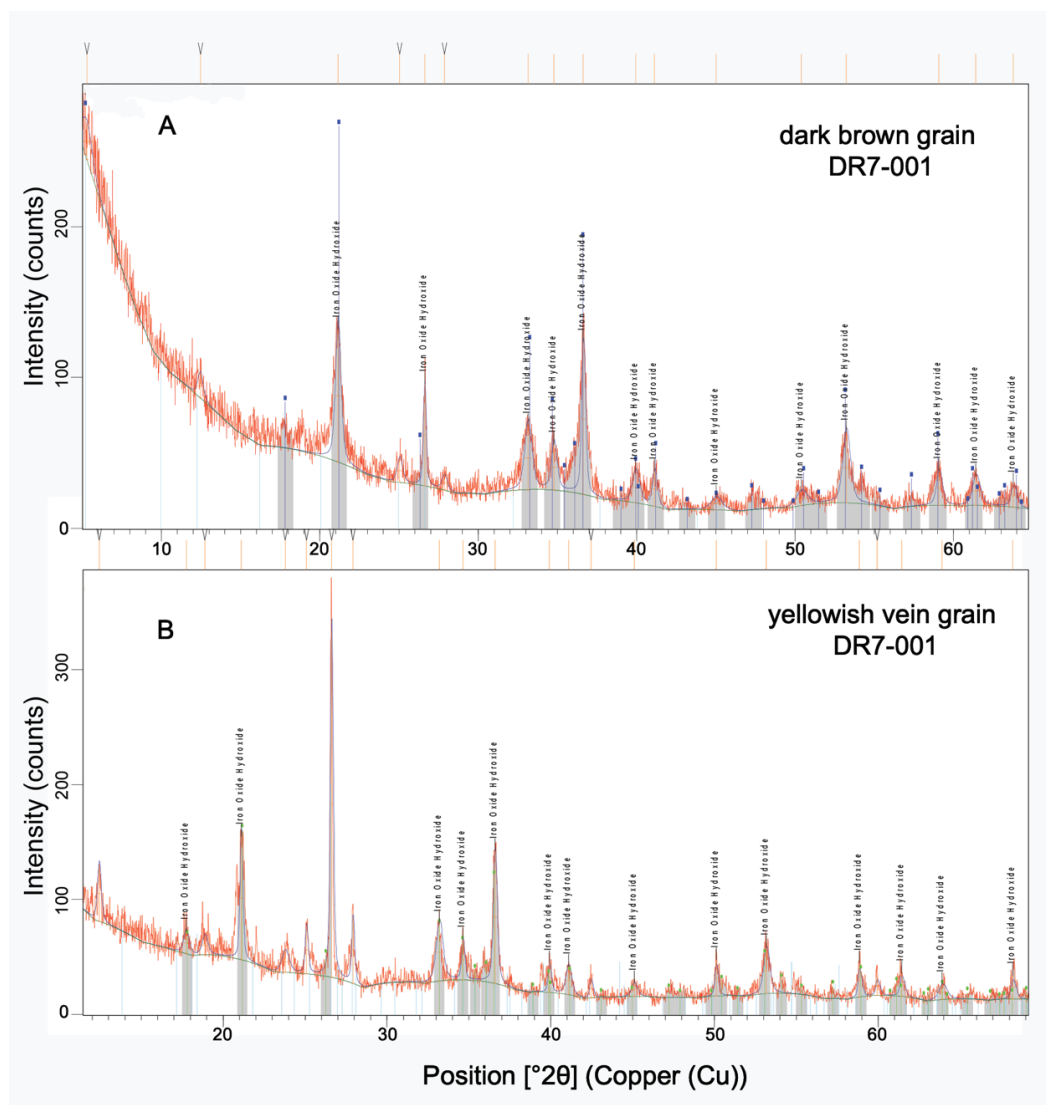
The Amerasia basin of the Arctic Ocean remains one of the Earth's least explored region (Brumley et al., 2015). The Chukchi Borderland and Mendeleev Ridge are known as Paleozoic continental blocks that occur within the Amerasia Arctic Ocean. During the U.S. and Russian research cruises fragments of Fe- and Mn-oxide mineralization were collected from several sites of the northern Chukchi Borderland and central Mendeleev Ridge (Fig. 1A; Hein et al., 2017; Konstantinova et al., 2017). The subject of this study is the age dating of samples from dredge haul DR7 collected from 3400 m water depth (coordinates 78.53N, 156.68W).

The DR7 dredge haul consists of rock fragments that are extensively altered and finely sheared. Two different rock types were found. First one shows alternating yellow-brown and dark-brown layers, with dendrites of the dark-brown material in the yellow-brown laminae (Fig. 1B). Both layer types mainly comprise Fe-(hydro)oxides, but the dark-brown layers have a higher Mn-oxide content. Another rock type in DR7 is a breccia with poorly sorted predominantly angular to subangular clasts (Fig. 1C), that include pure Fe oxyhydroxide, basalt, and altered metasedimentary rocks. Mn- or Fe-oxide are found in some larger clasts. The breccia cement is composed predominately of dark brown Fe-oxyhydroxides with submetallic grey areas. The microstructure varies from bladed to nodular to massive. The breccia is predominantly cement-supported, indicating replacement during Fe- and Mn-oxide mineralization. Based on morphology, structure, mineral and chemical composition especially high abundance of Fe-(hydro)oxides these samples differ from the widespread underwater hydrogenic Fe-Mn mineralization, and, likely have a hydrothermal origin (Hein et al., 2000).



75 **Figure 1. (A) Regional setting of the Amerasia Basin (inset) and location map of the DR7 dredge haul; (B) cut section images of the main sample types; all subsamples for age dating are from DR7-001.**

The dominant mineral in the mineralized samples based on X-ray diffractions is goethite and possibly lesser amounts of ferroxhyte (δ -FeOOH) and ferrihydrite [$\text{Fe}^{3+}_{4.5}(\text{OH},\text{O})_{12}$] (Table 1; Fig. 2). The darker colored goethite has better crystallinity than the paler ones.



80 **Figure 2. X-ray diffraction mineralogy of the dark brown clast (A), and yellow-brown vein material (B) from the DR7-001 sample. Iron Oxide Hydroxide peaks (marked grey) refers to the mineral goethite. The peaks of birnessite (MnO₂) and quartz are observed in both samples. The yellow-brown vein material also contains minor amounts of plagioclase, and, probably, illite.**

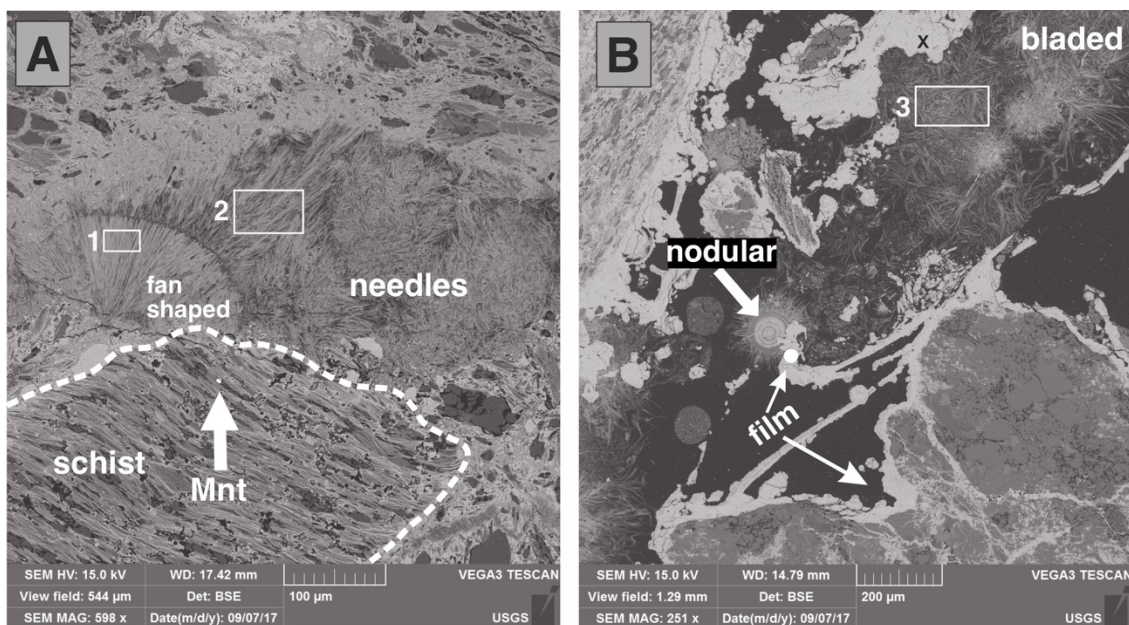
Based on SEM-EDS studies (Fig. 3) Fe-oxides crystallite sizes of cement and replacements vary from submicrometer to a few micrometers, rarely up to 120 µm. Birnessite and 10Å manganates (todorokite, busserite, or asbolane) and δ-MnO₂ (vernadite) occur as well. Relict host-rock minerals include quartz, feldspar, mica, and clay minerals. Clinocllore (chlorite) is ubiquitous in the DR7 samples. Among the U-bearing minerals, single grains of zircon and monazite were observed (Fig. 3).

Table 1. XRD Mineralogy of Crystalline Phases of DR7 Sample from the Amerasia Arctic Ocean.

Sample ID	Description	Major	Moderate	Minor
DR7-001-L1A	Cement from breccia	Goethite	Quartz, Birnessite	TAM
DR7-001-L1B	Glassy Fe-rich clast	Goethite	--	--
DR7-001-L2B	Fe-rich dark-brown lamina	Goethite, Birnessite	Clinocllore, Quartz, Plagioclase	δ-MnO ₂ , TAM
DR7-001-L2D	Reddish vein	Goethite, Quartz	Clinocllore, Plagioclase, Mica	Birnessite, TAM(?)
DR7-001-L2E	Fe-Mn lamina	Birnessite, Goethite	TAM(?), Quartz	Plagioclase

Major >25%, Moderate 5-25%, Minor <5%. TAM is 10Å Manganates = todorokite, busserite, or asbolane. Goethite may also include feroxyhyte or ferrihydrite.

90 Comment: X-ray diffraction mineralogy was completed using a Malvern Panalytical X'Pert Powder X-ray diffractometer (XRD) with CuKα radiation and graphite monochromator run from 4° to 70° 2θ with a step size of 0.02° 2θ at 40 kV and 45 mA at USGS, PCMSC lab in 2017. Digital scans were analyzed using Philips X'Pert High Score Plus software to analyze X-ray reflections and identify possible mineral phases.



95 **Figure 3.** Backscatter SEM photomicrograph images of sample DR7-001 and DR7-002 from polished thin sections; (A) fan-shaped (26% Fe, 17% Mn for box 1), needle (28% Fe, 15% Mn for box 2), and massive cements of Fe and Mn oxides in the breccia part of sample DR-001; note schist grain in the lower left quadrant with a bright monazite grain (Mnt); (B) cement of breccia: bladed (box 3: 29% Fe, 35% Mn), nodular (white arrow: 33% Fe, 25% Mn), and film type (white dot: 68% Fe; black x: 35% Fe, 29% Mn) Fe- and Mn-oxide cements; bladed cement consists of discrete Mn-oxide and Fe-oxyhydroxide blades, and Fe and Mn contents vary for each laminae in the micronodule.

100 Polished thin sections were carbon coated and used for SEM-EDX analyses of samples DR7-001 and DR7-002 using a Tescan Vega3 scanning electron microscope (SEM) at operating conditions of 30 kV and 15 nA for imaging; the Energy Dispersive Spectrometry (EDS) chemical characterization and element mapping was done using a JEOL 8900 operating at 15 kV and 40 nA for quantitative analyses of oxides; counting times were 30 s peak and 15 s background at USGS lab in Menlo Park in 2017.

3. Methodology and sampling strategy

105 For (U-Th)/He dating fragments of goethite mineralization were manually extracted from the DR7-001 sample: dark-brown clasts of breccia and yellow-brown vein material (Fig 1B). According to the SEM and XRD data samples mainly consist of pure crystalline goethite (Fig. 2,3) with possible admixture of birnessite and quartz. Therefore, the samples represent a standard material which is used for (U-Th)/He dating (Flowers et al., 2022). The low-temperature steady and deep underwater environment (~ 0°C) prevent thermal loss of He from the samples during their geological history.

3.1. Sample preparation

110 In order to exclude possible U-loss during the sample preparation when goethite grains are sonicated in a distilled water the leaching experiments were conducted. Millimetre-size fragments of goethite were manually extracted from the DR7-001

sample which represented dark-brown clast of the breccia and a yellow-brown vein material (Fig. 1B,C). At the first stage the massive single fragments in the closed Teflon vials with 3 ml of distilled deionized water (Barnsted) were sonicated for 15 min at room temperature without extra cooling. The solution was removed by the mechanical pipette for subsequent chemical
115 analyze. At the second stage the remained grains were dried at room temperature for 24 hours and crushed in the Teflon vial by the molybdenum stick ($< 300 \mu\text{m}$) to increase their specific surface area. The crushed grains were sonicated in distilled deionized water (Barnsted; 3 ml) for extra 15 min at room temperature without extra cooling. After the solutions were left for 24 hours for the sinking of the small floating particles. The uppermost 1 ml of the solution was carefully moved to a new beaker and nitric acid was added up to 5% HNO_3 solutions (50–150 μl). Uranium and Th contents were measured by
120 ELEMENT 2 ICP mass-spectrometer at the Institute of Precambrian Geology and Geochronology RAS. The full procedural blanks were obtained by the parallel procedures with an empty beaker. The total U and Th content of the sample was determined in the same way after its complete dissolution in the mixture of aqua regia (200 μl) with HF (250 μl) and HClO_4 (10 μl) for 15 h at 110°C in a closed Teflon vial in thermostat. Due to described analytical procedure the obtained U and Th contents in the leaching solutions are semi-quantitative.

125 3.2. (U-Th)/He dating

Eight millimeter-size fragments of goethite mineralization were manually extracted for (U-Th)/He dating from three different parts of the DR7-001 sample: two dark-brown clasts of the breccia and a yellow-brown vein from the completely altered rock (Fig. 1B,C; Table 2). Subsamples from the yellow-brown vein material and from dark-brown gains were treated as separate samples (1-8). Samples were derived from the inner part of the original sample, had no visible under the binocular microscope
130 inclusions of other minerals and were not washed.

3.2.1. Measurement of radiogenic ^4He contents

For each measurement, $\sim 1\text{--}3$ mg fragments of goethite grains were placed in a quartz ampoule (~ 1 cm long) and sealed under a 10^{-3} torr vacuum (Fig. 4). The sealing was done by the distilled water-based torch LIGA (Vasileostrovsky Electrochemical Plant). The torch has a narrow flame that prevent heating of the sample during the sealing. The Durango apatite ($n=3$) sealed
135 in a quartz ampoules by the same technique did not show any sign of He loss (Fig. S1). The sealed ampoule, via a special gateway, was placed in a high-temperature high-vacuum furnace of the magnetic sector MSU-G-01-M mass-spectrometer equipped with two SAES getter pumps (Spectron Analyt, IPGG RAS; Shukolyukov et al. 2012a,b). During heating, He easily diffuses through the thin quartz walls while U and other products of the sample decomposition remain in the ampoule. A Secondary Electron Multiplier (SEM) was used to determine the $^4\text{He}^+$ beam intensity (cps). Calibration of the mass

140 spectrometer was done using Knyaghinya meteorite (Schultz and Franke, 2004) and RS-Pt reference material (Yakubovich et al. 2023).

Goethite samples were step-heated at temperatures of 350° C for 30 min, 550° C for 10 min, 900° C for 10 min, 1100° C for 15 min, and 1150° C until He stop to release (5 min in average). Samples 1 and 2 (ID 966, 969, Table 2) were step-heated under slightly different conditions, starting with a temperature of 240° C. This step-heating approach allows for monitoring
145 the He release pattern from the goethite grains as well as the excess hydrogen (ion HD⁺) in the chamber of the mass-spectrometer. The diffusion of He through the thin quartz walls of the ampoule is fast (Shuster and Farley, 2005; Yakubovich et al., 2014), but it does not allow to obtain the accurate diffusion kinetics of He from the goethite grains.

Following the extraction of He, the ampoule was removed from the mass spectrometer for subsequent separation of U and Th. The total procedural blank, determined by heating the empty quartz ampoules to 1100°C, corresponds to $4.4 \pm 1.6 \times 10^{-10} \text{ cm}^3$
150 He at STP.

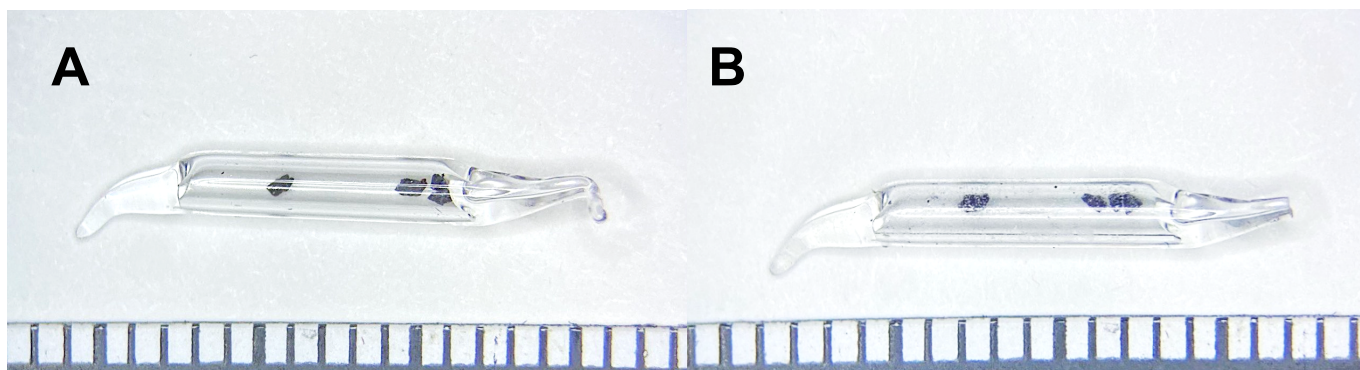


Figure 4. Fragments of goethite in a sealed quartz ampoule (A) before heating; (B) after heating. Scale bar 1 mm.

3.2.2. Measurement of U and Th Contents

155 The quartz ampoule with degassed samples was spiked with a ²³⁰Th-²³⁵U tracer and dissolved in a mixture of aqua regia (0.4 mL), concentrated hydrofluoric acid (0.5 mL), and perchloric acid (0.05 mL) in closed Teflon vials for 2 hours at 200° C on a hot plate followed by 15 h at 110° C in a thermostat. The solution was dried on a hot plate at 200° C. During this step, perchloric acid prevented the formation of low-soluble fluorine complexes, while most of Si evaporated in a form of SiF₄. The remaining precipitate was dissolved in 1.5 mL of 5% nitric acid and heated up to 80° C in an ultrasonic bath for 15 min prior the
160 measurement of U and Th contents. ²³⁵U/²³⁸U and ²³⁰Th/²³²Th isotope ratios were measured on an ELEMENT XR ICP mass-spectrometer at the Vernadsky Institute of Geochemistry and Analytical Chemistry RAS. The total chemical procedure blank,

determined by dissolution of the empty quartz ampoules (n=4) using the same settings, corresponds to 1.30 ± 1.26 and 5.8 ± 4.4 10^{10} atoms of ^{238}U and ^{232}Th respectively.

The (U-Th)/He ages were calculated using IsoplotR software (Vermeesch, 2018). The combined analytical uncertainty was estimated based on the U, Th, and He measurement uncertainties and the uncertainty based on the blank determinations. The alpha-recoil corrections were not applied, because all analyzed samples are the fragments of large grains.

Table 2. Results of (U-Th)/He Dating of Goethite Subsamples of DR7-001

No.	ID	Type	Mass [mg]	U [ppm]	U [10^{10} at]	σ [%]	Th [ppm]	Th [10^{10} at]	σ [%]	Th/U	$^4\text{He}^d$ [cm^3 STP g^{-1}]	^4He [10^{10} at]	σ [%]	age [Ma]	2σ
1	966		0.954	2.51	603	1.8	0.81	194	3.6	0.3	2.9×10^{-6}	7.54	2.3	9.1	0.5
2 ^a	969	Dark grains	7.197	1.86	3376	1.1	0.69	1258	2.1	0.4	3.4×10^{-6}	65.17	2.8	13.8	0.8
3	1015		1.946	2.62	1287	1.3	0.66	323	1.8	0.3	2.6×10^{-6}	13.73	3.7	7.9	0.6
4	1022		1.908	2.78	1338	1.8	0.81	387	2.0	0.3	3.1×10^{-6}	15.97	3.2	8.7	0.6
5 ^a	1031		2.973	2.43	1823	2.8	1.99	1491	2.4	0.8	4.3×10^{-6}	33.99	2.8	12.2	0.9
6	1032		3.115	2.25	1769	5.2	1.76	1379	5.0	0.8	2.6×10^{-6}	21.85	2.7	8.2	0.8
Dark brown grains weighted mean^c 8.6 ± 0.3															
7	1033	Vein grains	1.782	1.36	613	2.2	3.30	1481	1.6	2.4	1.1×10^{-6}	5.40	8.7	4.4	0.8
8	1036		2.708	1.80	1232	2.5	4.90	3347	1.9	2.7	1.8×10^{-6}	12.70	3.9	4.9	0.4
Yellowish brown vein weighted mean^c 4.8 ± 0.4															
	Empty Quartz ampoule ^b		28–56	--	1.3	97	--	6	74	--	--	1.1	37	--	--

The reported uncertainties of U, Th, and He measurements are the combined uncertainties calculated by summation in quadrature of measurement and blank uncertainties using a coverage factor of 1 which gives a level of confidence of approximately 65%.

^aNo. 2 and 5 ages not used in the calculation of mean age; see text in Results section for explanation.

^bContents of U, Th, and He in the quartz ampoule represent full analytical blank, which includes chemistry and steps of sample preparation (sealing, heating).

^cThe reported uncertainties of an age value is an expanded analytical uncertainty which include analytical uncertainty of U, Th, He measurements and factors addressed at the section 4.2. Error value corresponds to 95% level of confidence (2σ).

^dThe calibration of the mass-spectrometer was done using the mineral reference materials in a range of He content from 2 to 200 [10^{10} at].

Table 3. Results of the leaching experiments of Goethite Subsamples of DR7-001

Sample	Stage	Weight, mg	U, ng	Th, ng	Th/U	Fraction of U-loss	Fraction of Th-loss
dark grain	first	5.628	0.03	0.01	0.26	0.3	0.3
	second		0.38	0.02	0.06	3.5	0.6
	residual		10.7	3.4	0.32	-	-
dark grain-2*	second	2.462	0.03	0.02	0.6	0.5	0.23
	residual		5.4	7.3	1.3	-	-
vein grain	first	6.212	0.01	0.02	1.4	0.12	0.10
	second		0.6	0.40	0.6	7.8	1.6
	total		8.4	24.7	2.5	-	-
vein grain-2*	second	1.890	0.11	0.19	1.7	3.0	1.7
	residual		3.6	10.9	3.0	-	-
blank	first	-	0.004	0.002	0.5	-	-
	second		0.01	0.005	0.7	-	-
	residual		0.01	0.02	1.8	-	-

180

Comment: * grains were crushed and sonicated without previous step (first stage).

4. Results

185 4.1. Leaching experiments

Chemical analyses of the distilled water leachates revealed the partial loss of U and Th from the subsamples (Table 3). The leaching of U and Th from the crushed subsample is more intensive than from a massive grain and reach up to 8% for U and less than 2% for Th. Because the samples are not water soluble but the leachates contain also some amount of Mn, Fe and Co, some tiny floating particles of the original sample might be in the solution. The ICP-MS measurements were calibrated only for U and Th, thus quantification of the number of floating particles in the solution based on Fe and Mn content is not possible. However, the notable shift of the Th/U ratio in the solution relative to the Th/U ratio of the residual goethite (from 0.06 to 3; Table 3) indicates that some part of U was leached from the samples. These findings are in an agreement with previous results of Fe- and Mn-oxides leaching experiments by a weak acids with acetate buffer (Konstantinova et al., 2018; Koschinsky and Hein, 2003) which implies U and Th adsorbed behavior.

195 4.2. (U-Th)/He dating results

The (U-Th)/He ages for eight fragments of goethite from sample DR-7-001 included fragments of two sets of dark grains from two separate breccia goethite clasts (grains 1-4 and 5-6) and one set of yellow-brown vein samples (grains 7-8) (Table 2; Fig. 5). The signals of He, U, and Th of all samples were markedly higher than the background level (empty quartz ampoule). The concentrations of U in the dark goethite grains range from 2.2–2.8 ppm, with Th/U ratios of 0.3–0.8. The concentration of U in the two vein subsamples is lower (1.36 and 1.8 ppm) and Th prevails over U (Th/U 2.4–2.7). Concentrations of ^4He range from 2.6 to 4.3 x 10⁻⁶ cm³ STP g⁻¹ for the dark-brown grains and from 1.1 to 1.8 x 10⁻⁶ cm³ STP g⁻¹ for vein samples. Among

200

the six dark goethite grains analyzed, one had an atypically low U concentration (1.86 ppm; Table 2). Sample 5 (ID 1031) had an unusual high-temperature He release pattern ($>1100^\circ$, Fig. 7), which likely indicates the presence of He-retentive mineral inclusions. These anomalous samples (ID 969; 1031) revealed (U-Th)/He age in a range of 12.2–13.8 Ma (Table 2). This coincidence might indicate that we are wrong when consider these measurements as erroneous. However, in a lack of confidence we are not going to interpretate this age value.

The (U-Th)/He age of the remaining dark grains is consistent within the uncertainty of the measurements with a weighted mean value of 8.6 ± 0.3 Ma (2σ). The two yellow-brown vein samples had significantly younger reproducible ages, with a mean of 4.8 ± 0.4 Ma (2σ).

210

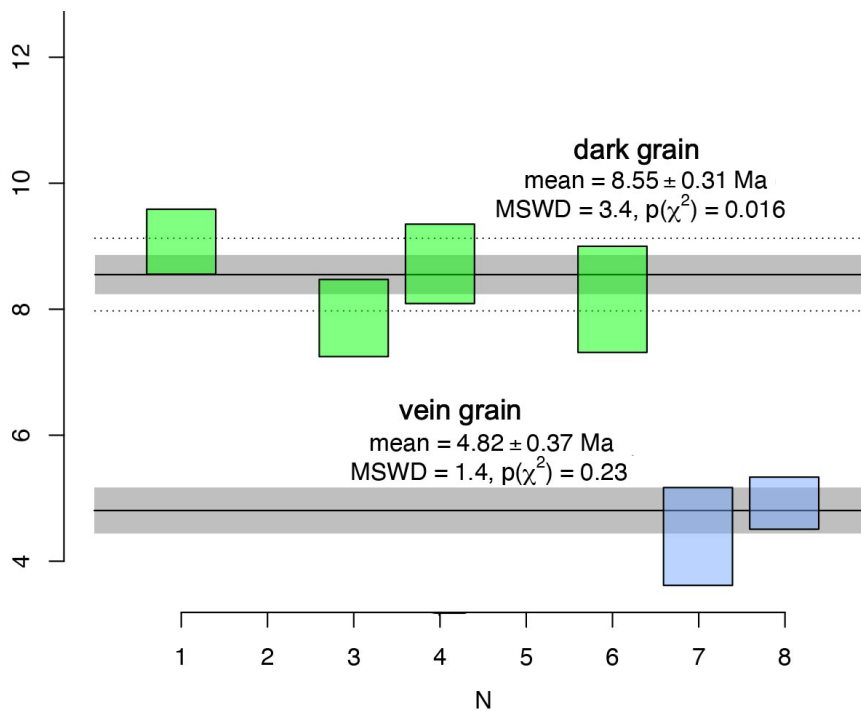


Figure 5. Results of (U-Th)/He dating of goethite from DR7-001 subsamples. Error bars 2σ . Weighted mean plot constructed using IsoplotR software (Vermeesch, 2018).

5. Discussion

215 5.1. Methodological implications

5.1.1. Sample preparation

Due to the leaching experiments around 8% of U and 1.7% of Th can be remobilised from the sample by the fresh deionized distilled water, which is known to become chemically active after the contact with atmosphere (pH 5–6; Gurr, 1962). Goethite is not a water-soluble mineral therefore U release likely indicates its position beyond the crystal lattice or in some unstable
220 phases. Th/U ratios of the grains (0.3 and 1.3 for dark grains; 2.5 and 3.0 for a vein material) are remarkably higher than those of leachates (0.06 and 0.6; 0.6 and 1.7, respectively; Table 3), which implies that U is easier to mobilize. This is in favor of the adsorbed form of some of the U, rather than the presence of unstable phases with different Th/U ratios. The higher percent of U-loss from the crushed samples is also in agreement with this suggestion (Table 3).

The possible adsorbed behavior of U in goethite from the weathering environment was discussed by Shuster et al (2005) and
225 Vasconcelos et al. (2013). The leaching experiments are also in agreement with the results of radiochemical experiments that revealed that during the crystallization of hematite and goethite from ferrihydrite (Fe^{3+})₂O₃·0.5H₂O, which is the least stable iron (oxyhydr)oxide, only part of uranium becomes leaching-resistant (Payne et al., 1994).

The proportion of U in adsorbed form relative to the U, which is incorporated into crystal lattice can differ from sample to sample. This is indirectly confirmed by the discussion in Vasconcelos et al. (2013), which suggest that various patterns of U-
230 loss during the He release from the goethite samples possibly indicated different U position of the analyzed samples. Adsorbed behavior of some of the U does not affect strongly on applicability of the (U-Th)/He method due to the long alpha-stopping distances (Shuster et al., 2005). However, sonication of the samples in distilled water prior (U-Th)/He dating might result in U-loss and subsequent erroneous/over-dispersed ages of multi-mineral grains. Large grains are unlikely to lose the significant amount of U as their surface to volume ratio is low.

235

5.1.2. Justification of the technique

(U-Th)/He ages of goethite subsamples are reproducible. Measured concentration of U in the samples which were degassed in the quartz ampoules (1.4–2.8 ppm; Table 2) are in a range of their concentrations in the unheated grains (1.5–2.5 ppm; n=5; ICP MS). This indicates that the proposed analytical approach is well suited for (U-Th)/He dating of goethite, and likely other
240 Fe-(oxyhydro)oxides. Encapsulating the individual goethite grains into the quartz ampoule exclude any U-loss during the sample degassing which is one of the major analytical concerns (Vasconcelos et al., 2013; Hofmann et al., 2020; Wu et al., 2019). The approach allows overheating of the sample with plenty of reserve. Based on our experience on He release from isoferroplatinum (Pt₃Fe) quartz ampoules are robust to temperatures up to 1450°C (Shukolyukov et al., 2012b). One of the

245 main disadvantages of the proposed technique is the relatively high blank of the quartz ampoule, which complicates analyse
of very small and/or grains that are too young. The technique is quite sufficient for (U-Th)/He dating of mg-weighted samples
of Neogene age as tested here, and require remarkably lower amount of the material than double- or multi aliquot approaches
(Pidgeon et al., 2004; Wu et al., 2019). The technique also does not require the modernisation of the He extraction line which
is needed for the degassing in the presence of O₂ (Hofmann et al., 2020).

250 **5.1.3. Future developments**

We suggest that application of the same technique on other mass-spectrometers might result in even better reproducibility of
the (U-Th)/He ages of goethite samples. The secondary electron multiplier of the MSU-G-01-M mass-spectrometer has a
reproducibility in a range of around 2.5%, application of these technique on the instruments equipped with a Faraday cup,
which have better reproducibility (~1.2%; Yakubovich et al. 2023), might have produce even better values.

255 In order to determine the analytical limitations of the proposed methodological approach additional test and improvements
could be done in the future as well.

- (1) Dating washed samples to test if the U-leaching results in systematically older ages and quantify its impact on the
overdispersion of (U-Th)/He ages;
 - (2) Dating Fe-(oxyhydro)xides with independent age constraints in order to confirm the reability of the procedure;
 - 260 (3) Heating grains to higher temperatures to ensure complete helium release;
 - (4) Demonstrating complete recovery of volatilized U by comparing the results presented here to U and Th measurements
on unheated aliquots;
 - (5) Measure a comprehensive set of Durango apatite grains by the same technique in order to confirm the absence of He
lost by the grains during the sealing procedure.
- 265 Pre-screening the grains for inclusions with micro-CT in order to avoid grains with the inclusions of other minerals would also
improve the suggested methodological approach.

5.2 Geological implications

The results of the (U-Th)/He age dating of goethite grains from the slope of Chukchi Borderland produce a Neogene age
formation. There are several factors that might potentially affect the mineral age results, such as He loss, radiation damage,
270 recrystallisation, and fluid and mineral inclusions, which we discuss below.

5.2.1. Helium thermal retentivity

Goethite is predominantly He retentive under surface conditions (Cooperdock and Ault, 2020). The mineral is able to retain around 80–95% of its radiogenic ^4He for millions of years (Shuster et al. 2005; Deng et al. 2017; Hofmann et al., 2017). The water temperature at 3400 m water depth within Chukchi Borderland slope is about $-0.3\text{ }^\circ\text{C}$ (Zhang et al., 2021), therefore any thermal loss of He seems unlikely, though it could be induced by local hydrothermal events.

Heating the sample in a quartz ampoule does not allow the measurement of the He diffusion parameters, nevertheless it does reflect the He retentivity of the sample. Despite different He release patterns (Fig. 6) the (U-Th)/He age of the same group is quite uniform, which likely indicates insignificant thermal loss of ^4He (Fig. 6). Remarkable that He release pattern of the sample 3 (ID 1015) significantly differs from the patterns of the other grains, despite its (U-Th)/He age is consistent with other measurements.

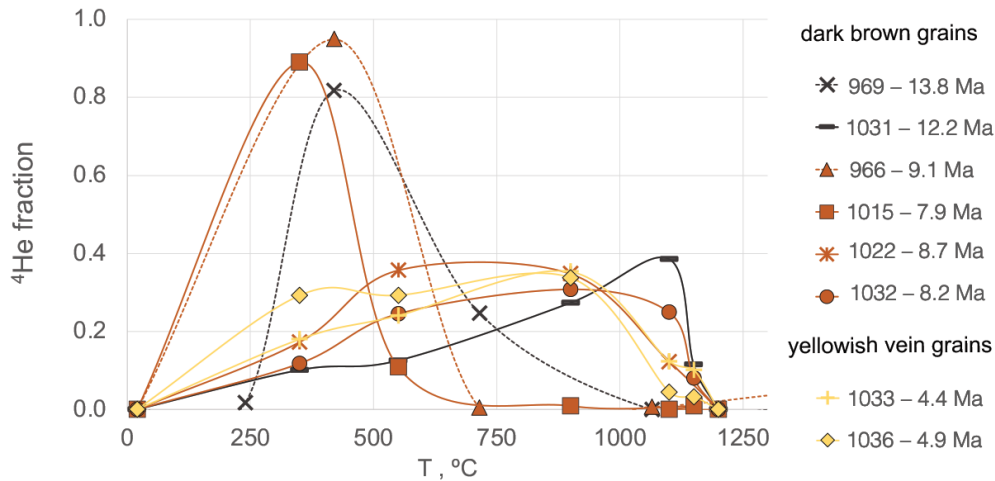


Fig. 6. Helium release pattern from the mainly (>95%) goethite grains sealed in Quartz ampoule. All measurements (with the exception of the samples 966 and 969; dotted line) were carried out under the same time-temperature conditions. Values are a sample ID in the Table 2.

5.2.2. Radiation damage

The He loss from goethite is strongly controlled by radiation damage, for example radiogenic defects and some other impurities (e.g., Al) decrease the ability of He to diffuse (Bassal et al., 2022). The samples has close modern eU content and in the limited range of its variation there is no correlation with (U-Th)/He age values (Fig. 7). The uniform (U-Th)/He ages of the petrological groups (clasts and vein) indicate limited impact of the radiation damage on the dispersion of He ages.

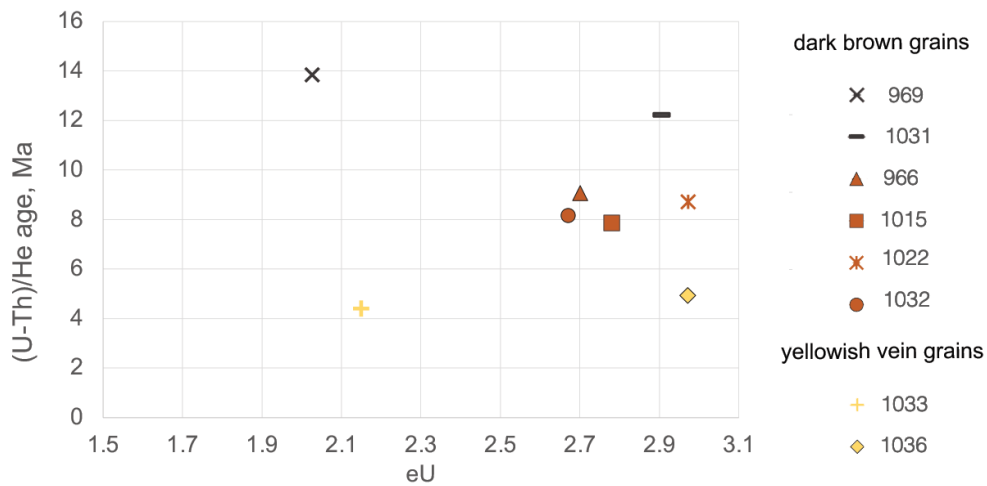


Figure 7. Goethite (U-Th)/He ages versus eU concentration of the samples. The effective modern uranium concentration (eU) was calculated based on the formulas given by (Flowers et al., 2023). Index is a sample ID in the Table 2.

5.2.3. Mineral and fluid inclusions and impurities

295 The studied samples contain rare U- and Th-rich mineral inclusions, such as zircon and monazite, with sizes ranging between < 1 to 40 μm (e.g. Fig. 3). If there was incomplete dissolution within the chemical procedure, the U-loss would result in an erroneously old and unreproducible ages, which might be the case of sample 5 (ID 1031).

Helium concentration of minerals fluid inclusions that formed during magmatic and hydrothermal processes typically does not exceed $10^{-8} \text{ cm}^3 \text{ STP g}^{-1}$ (Stuart et al., 1994; Graupner et al., 2006), that is less than 1% of the total He of the studied samples
 300 and insignificant for our (U-Th)/He dating procedure.

Incorporation of Sm can be an additional source of ^4He in goethite. Sm contents of the DR7-001 samples vary from 5.5 to 6 ppm (ICP-MS data; lithium-metaborate fused disks; $n=3$), which implies that Sm would produce less than 0.25% of the He sample budget.

XRD data indicates that goethite from the yellow-brown vein material has lower crystallinity and higher abundance of mineral
 305 inclusions such as quartz, plagioclase and illite (Fig. 2; Table 1). These factors potentially might decrease the (U-Th)/He age of the samples. Thus, we cannot exclude that the younger age of the goethite from the yellow-brown vein is related to some He-loss.

5.2.4. Recrystallization

310 Goethite is the most thermodynamically stable Fe-(oxy)hydroxide in the near-surface environment. However, it can undergo
dissolution–recrystallization processes during interaction with acidic solutions that reset its (U-Th)/He age (Monteiro et al.,
2014). These processes enrich samples with low-soluble components that increase the Th/U ratios. This might be initiated by
the presence of Fe²⁺ ions in the aquatic systems (Handler et al., 2014). Given that the vein has higher Th/U ratios (2.5–2.7 vs
0.3–0.8 of the dark grains) and younger (U-Th)/He age (4.8±0.9 Ma vs 8.6±1.2 Ma; Table 2), its newly formation due to the
recrystallization of goethite cannot be ruled out.

315 5.2.5. Interpretation of (U-Th)/He ages

In additional to assessment of the all factors that might impact the (U-Th)/He ages, we include 10% (2σ) uncertainty to the
primary analytical uncertainty of the measurements based on the suggestion of (Monteiro et al., 2014). Thus, the dense dark-
brown goethite have the age of 8.6±1.2 Ma (2σ), and the vein material is younger, 4.8±0.9 Ma (2σ). These values do not
overlap within the extended uncertainty.

320 The (U-Th)/He ages reflect the time of mineral formation, recrystallization, or cooling below the closure temperature. Closure
temperature of goethite varies over a wide range, from ~20 to 150° C, depending on the diffusion domain sizes and distribution
of the defects in the crystal lattice (Bassal et al., 2022). Thus, the uniform (U-Th)/He ages of the dark-brown grains
accompanied by remarkably different He release patterns (Fig. 6) might be explained by cooling, only with the assumption of
fast (1–2 Ma) host rocks uplift from ~2–4 km depth that took place ~9 Ma ago. However, that assumption is inconsistent with
325 the tectonic evolution of the Arctic region (e.g., Chian et al., 2016; Craddock and Houseknecht, 2016). Therefore, (U-Th)/He
ages of the dark grains of pure crystalline goethite reflect a Neogene mineralization event in the Chukchi Borderland, Arctic
Ocean. More data is required in order to check the possible presence of fragments of older Fe- and Mn- mineralised rocks (12–
14 Ma; Table 2), as well as to confirm the young (~ 4.8 Ma) mineralization event.

6. Conclusion

330 Reproducible (U-Th)/He ages is achieved using our proposed analytical approach, which involves sealing the sample in quartz
ampoule for He release is well suited for (U-Th)/He dating of Fe-(oxy)hydroxides; this techniques allows for the determination
of U, Th, and He on the same subsample aliquot. Our data also indicate a fraction of U can be leached from multi-grain goethite
samples during sonication in the distilled water, implying that this step of goethite sample preparation for (U-Th)/He dating
should be taken with caution.

335

(U-Th)/He ages of goethite from the slope of the Chukchi Borderland formed during a Neogene mineralization event (8.6 ± 1.2 Ma). The younger age of the yellow-brown vein material (4.8 ± 0.9 Ma) can be explained by an episode of later-stage mineralization, recrystallization or by its lower crystallinity. Alternatively, the small number of dated samples and distribution of samples may preclude being able to detect continuous Neogene mineralization throughout the region. Further investigations and a larger sample set are recommended for a comprehensive understanding of the geological evolution of the region.

Competing interests

The contact author has declared that none of the authors has any competing interest.

Acknowledgements

We thank James R. Hein and Kira Mizell from U.S. Geological Survey for the provision of samples used in this study and for reviews. We are grateful to Irina Volkova (Department of crystallography; Saint Petersburg State University) for the assistance. Xiao-Dong Deng, Florian Hofmann, Hevelyn S. Monteiro, Marissa Tremblay, Cecile Gautheron are gratefully acknowledged.

This research was supported by RSF 22-77-10088. Chemical analyses done by M.O. Anosova were funded by the State Assignment of the Vernadsky Institute of Geochemistry and Analytical Chemistry, Russian Academy of Sciences.

References

- 350 Ansart, C., Quantin, C., Calmels, D., Allard, T., Roig, J. Y., Coueffe, R., Heller, B., Pinna-Jamme, R., Nouet, J., Reguer, S., Vantelon, D., and Gautheron, C.: (U-Th)/He Geochronology Constraints on Lateritic Duricrust Formation on the Guiana Shield, *Front. Earth Sci.*, 10, 1–19, <https://doi.org/10.3389/feart.2022.888993>, 2022.
- Bassal, F., Heller, B., Roques, J., Balout, H., Tassan-Got, L., Allard, T., and Gautheron, C.: Revealing the radiation damage and Al-content impacts on He diffusion in goethite, *Chem. Geol.*, 611, <https://doi.org/10.1016/j.chemgeo.2022.121118>, 2022.
- 355 Basu, S., Stuart, F. M., Klemm, V., Korschinek, G., Knie, K., and Hein, J. R.: Helium isotopes in ferromanganese crusts from the central Pacific Ocean, *Geochim. Cosmochim. Acta*, 70, 3996–4006, <https://doi.org/10.1016/j.gca.2006.05.015>, 2006.
- Benites, M., Hein, J. R., Mizell, K., Farley, K. A., Treffkorn, J., and Jovane, L.: Geochemical insights into formation of enigmatic ironstones from Rio Grande rise, South Atlantic Ocean, *Mar. Geol.*, 444, 106716, <https://doi.org/10.1016/j.margeo.2021.106716>, 2022.
- 360 Brumley, K., Miller, E. L., Konstantinou, A., Grove, M., Meisling, K. E., and Mayer, L. A.: First bedrock samples dredged from submarine outcrops in the Chukchi Borderland, Arctic Ocean, *Geosphere*, 11, 76–92, <https://doi.org/10.1130/GES01044.1>, 2015.

- Chian, D., Jackson, H. R., Hutchinson, D. R., Shimeld, J. W., Oakey, G. N., Lebedeva-Ivanova, N., Li, Q., Saltus, R. W., and Mosher, D. C.: Distribution of crustal types in Canada Basin, Arctic Ocean, *Tectonophysics*, 691, 8–30, 365 <https://doi.org/10.1016/j.tecto.2016.01.038>, 2016.
- Cooperdock, E. H. G. and Ault, A. K.: Iron oxide (U-Th)/he thermochronology: New perspectives on faults, fluids, and heat, *Elements*, 16, 319–324, <https://doi.org/10.2138/gselements.16.5.319>, 2020.
- Craddock, W. H. and Houseknecht, D. W.: Cretaceous-Cenozoic burial and exhumation history of the Chukchi shelf, offshore Arctic Alaska, *Am. Assoc. Pet. Geol. Bull.*, 100, 63–100, <https://doi.org/10.1306/09291515010>, 2016.
- 370 Deng, X. D., Li, J. W., and Shuster, D. L.: Late Mio-Pliocene chemical weathering of the Yulong porphyry Cu deposit in the eastern Tibetan Plateau constrained by goethite (U–Th)/He dating: Implication for Asian summer monsoon, *Earth Planet. Sci. Lett.*, 472, 289–298, <https://doi.org/10.1016/j.epsl.2017.04.043>, 2017.
- Farley, K. a. and Stockli, D. F.: (U-Th)/He Dating of Phosphates: Apatite, Monazite, and Xenotime, *Rev. Mineral. Geochemistry*, 48, 559–577, <https://doi.org/10.2138/rmg.2002.48.15>, 2002.
- 375 Flowers, R. M., Zeitler, P. K., Danišik, M., Reiners, P. W., Gautheron, C., Ketcham, R. A., Metcalf, J. R., Stockli, D. F., Enkelmann, E., and Brown, R. W.: (U-Th)/ He chronology : Part 1 . Data , uncertainty , and reporting, *GSA Bull.*, 1–33, <https://doi.org/10.1130/B36266.1/5590022/b36266.pdf>, 2022.
- Flowers, R. M., Zeitler, P. K., Danišik, M., Reiners, P. W., Gautheron, C., Ketcham, R. A., Metcalf, J. R., Stockli, D. F., Enkelmann, E., and Brown, R. W.: (U-Th)/He chronology: Part 1. Data, uncertainty, and reporting, *Bull. Geol. Soc. Am.*, 135, 380 104–136, <https://doi.org/10.1130/B36266.1>, 2023.
- Graupner, T., Niedermann, S., Kempe, U., Klemd, R., and Bechtel, A.: Origin of ore fluids in the Muruntau gold system: Constraints from noble gas, carbon isotope and halogen data, *Geochim. Cosmochim. Acta*, 70, 5356–5370, <https://doi.org/10.1016/j.gca.2006.08.013>, 2006.
- Gurr, E.: Effect of heat on the pH of water and aqueous dye solutions, *Nature*, 4847, 1199–1200, 1962.
- 385 Handler, R. M., Frierdich, A. J., Johnson, C. M., Rosso, K. M., Beard, B. L., Wang, C., Latta, D. E., Neumann, A., Pasakarnis, T., Premaratne, W. A. P. J., and Scherer, M. M.: Fe(II)-catalyzed recrystallization of goethite revisited, *Environ. Sci. Technol.*, 48, 11302–11311, <https://doi.org/10.1021/es503084u>, 2014.
- Hein, J.R., Koschinsky, A., Bau, M., Manheim, F.T., Kang, J.-K., Roberts, L.: Cobalt-rich ferromanganese crusts in the Pacific, in: Cronan, D.S. (Ed.) *Handbook of marine mineral deposits*. pp. 239-279, 2000.
- 390 Hein, J. R., Konstantinova, N., Mikesell, M., Mizell, K., Fitzsimmons, J. N., Lam, P. J., Jensen, L. T., Xiang, Y., Gartman, A., Cherkashov, G., Hutchinson, D. R., and Till, C. P.: Arctic Deep Water Ferromanganese-Oxide Deposits Reflect the Unique Characteristics of the Arctic Ocean, *Geochemistry, Geophys. Geosystems*, 18, 3771–3800, <https://doi.org/10.1002/2017GC007186>, 2017.
- Heller, B. M., Riffel, S. B., Allard, T., Morin, G., Roig, J. Y., Couëffé, R., Aertgeerts, G., Derycke, A., Ansart, C., Pinna-

- 395 Jamme, R., and Gautheron, C.: Reading the climate signals hidden in bauxite, *Geochim. Cosmochim. Acta*, 323, 40–73, <https://doi.org/10.1016/j.gca.2022.02.017>, 2022.
- Hofmann, F., Reichenbacher, B., and Farley, K. A.: Evidence for >5 Ma paleo-exposure of an Eocene–Miocene paleosol of the Bohnerz Formation, Switzerland, *Earth Planet. Sci. Lett.*, 465, 168–175, <https://doi.org/10.1016/j.epsl.2017.02.042>, 2017.
- Hofmann, F., Treffkorn, J., and Farley, K. A.: U-loss associated with laser-heating of hematite and goethite in vacuum during
400 (U–Th)/He dating and prevention using high O₂ partial pressure, *Chem. Geol.*, 532, 119350, <https://doi.org/10.1016/j.chemgeo.2019.119350>, 2020.
- Konstantinova, N., Cherkashov, G., Hein, J. R., Mirão, J., Dias, L., Madureira, P., Kuznetsov, V., and Maksimov, F.: Composition and characteristics of the ferromanganese crusts from the western Arctic Ocean, *Ore Geol. Rev.*, 87, 88–99, <https://doi.org/10.1016/j.oregeorev.2016.09.011>, 2017.
- 405 Konstantinova, N., Hein, J. R., Gartman, A., Mizell, K., Barrulas, P., Cherkashov, G., Mikhailik, P., and Khanchuk, A.: Mineral phase-element associations based on sequential leaching of ferromanganese crusts, *Amerasia Basin Arctic ocean, Minerals*, 8, <https://doi.org/10.3390/min8100460>, 2018.
- Koschinsky, A. and Hein, J. R.: Uptake of elements from seawater by ferromanganese crusts: Solid-phase associations and seawater speciation, *Mar. Geol.*, 198, 331–351, [https://doi.org/10.1016/S0025-3227\(03\)00122-1](https://doi.org/10.1016/S0025-3227(03)00122-1), 2003.
- 410 Monteiro, H. S., Vasconcelos, P. M., Farley, K. A., Spier, C. A., and Mello, C. L.: (U–Th)/He geochronology of goethite and the origin and evolution of cangas, *Geochim. Cosmochim. Acta*, 131, 267–289, <https://doi.org/10.1016/j.gca.2014.01.036>, 2014.
- Payne, T. E., Davis, J. A., and Waite, T. D.: Uranium Retention by Weathered Schists - The Role of Iron Minerals, *Radiochim. Acta*, 66–67, 297–304, <https://doi.org/10.1524/ract.1994.6667.special-issue.297>, 1994.
- 415 Pidgeon, R. T., Brander, T., and Lippolt, H. J.: Late Miocene (U+Th)-4He ages of ferruginous nodules from lateritic duricrust, Darling Range, Western Australia, *Aust. J. Earth Sci.*, 51, 901–909, <https://doi.org/10.1111/j.1400-0952.2004.01094.x>, 2004.
- Reiners, P. W., Chan, M. A., and Evenson, N. S.: (U–Th)/He geochronology and chemical compositions of diagenetic cement, concretions, and fracture-filling oxide minerals in mesozoic sandstones of the Colorado Plateau, *Bull. Geol. Soc. Am.*, 126, 1363–1383, <https://doi.org/10.1130/B30983.1>, 2014.
- 420 Riffel, S. B., Vasconcelos, P. M., Carmo, I. O., and Farley, K. A.: Goethite (U–Th)/He geochronology and precipitation mechanisms during weathering of basalts, *Chem. Geol.*, 446, 18–32, <https://doi.org/10.1016/j.chemgeo.2016.03.033>, 2016.
- Schultz, L. and Franke, L.: Helium, neon and argon in meteorites: A data collection, *Meteorit. Planet. Sci.*, 39, 1889–1890, 2004.
- Shukolyukov, Y. A., Yakubovich, O. V., Yakovleva, S. Z., Sal'nikova, E. B., Kotov, A. B., and Rytsk, E. Y.:
425 Geothermochronology based on noble gases: III. Migration of radiogenic He in the crystal structure of native metals with applications to their isotopic dating, *Petrology*, 20, 1–20, <https://doi.org/10.1134/S0869591112010043>, 2012a.

- Shukolyukov, Y. A., Yakubovich, O. V., Mochalov, A. G., Kotov, A. B., Sal'nikova, E. B., Yakovleva, S. Z., Korneev, S. I., and Gorokhovskii, B. M.: New geochronometer for the direct isotopic dating of native platinum minerals (^{190}Pt - ^4He method), *Petrology*, 20, 491–505, <https://doi.org/10.1134/S0869591112060033>, 2012b.
- 430 Shukolyukov, Y. A., Yakubovich, O. V., Mochalov, A. G., Kotov, A. B., Sal'nikova, E. B., Yakovleva, S. Z., Korneev, S. I., and Gorokhovskii, B. M.: New geochronometer for the direct isotopic dating of native platinum minerals (^{190}Pt - ^4He method), *Petrology*, 20, 491–505, <https://doi.org/10.1134/S0869591112060033>, 2012c.
- Shuster, D. L. and Farley, K. A.: Diffusion kinetics of proton-induced He in quartz, *Geochim. Cosmochim. Acta*, 69, 2349–2359, <https://doi.org/10.1016/j.gca.2004.11.002>, 2005.
- 435 Shuster, D. L., Vasconcelos, P. M., Heim, J. A., and Farley, K. A.: Weathering geochronology by (U-Th)/He dating of goethite, *Geochim. Cosmochim. Acta*, 69, 659–673, <https://doi.org/10.1016/j.gca.2004.07.028>, 2005.
- Strutt, R.: Helium and Radio-activity in Rare and Common Minerals, *Proc. R. Soc. London. Ser. A, Contain. Pap. a Math. Phys. Character*, 80, 572–594, 1908.
- Strutt, R.: The Accumulation of Helium in Geological Time, *Proc. R. Soc. London. Ser. A, Contain. Pap. a Math. Phys. Character*, 83, 298–301, 1909.
- 440 Stuart, F. M., Turner, G., Duckworth, R. C., and Fallick, A. E.: Helium isotopes as tracers of trapped hydrothermal fluids in ocean-floor sulfides, *Geology*, 22, 823–826, [https://doi.org/10.1130/0091-7613\(1994\)022<0823:HIATOT>2.3.CO;2](https://doi.org/10.1130/0091-7613(1994)022<0823:HIATOT>2.3.CO;2), 1994.
- Vasconcelos, P. M., Heim, J. A., Farley, K. A., Monteiro, H., and Waltenberg, K.: $^{40}\text{Ar}/^{39}\text{Ar}$ and (U-Th)/He - $^4\text{He}/^3\text{He}$ geochronology of landscape evolution and channel iron deposit genesis at Lynn Peak, Western Australia, *Geochim. Cosmochim. Acta*, 117, 283–312, <https://doi.org/10.1016/j.gca.2013.03.037>, 2013.
- 445 Verhaert, M., Gautheron, C., Dekoninck, A., Vennemann, T., Pinna-Jamme, R., Mouttaqi, A., and Yans, J.: Unravelling the Temporal and Chemical Evolution of a Mineralizing Fluid in Karst-Hosted Deposits: A Record from Goethite in the High Atlas Foreland (Morocco), *Minerals*, 12, <https://doi.org/10.3390/min12091151>, 2022.
- Vermeesch, P.: IsoplotR: A free and open toolbox for geochronology, *Geosci. Front.*, 9, 1479–1493, <https://doi.org/10.1016/j.gsf.2018.04.001>, 2018.
- 450 Wernicke, R. S. and Lippolt, H. J.: Botryoidal hematite from the Schwarzwald (Germany)" heterogeneous uranium distributions and their bearing on the helium dating method, 114, 287–300, 1993.
- Wu, L. Y., Stuart, F. M., Di Nicola, L., Heizler, M., Benvenuti, M., and Hu, R. Z.: Multi-aliquot method for determining (U + Th)/He ages of hydrothermal hematite: Returning to Elba, *Chem. Geol.*, 504, 151–157, <https://doi.org/10.1016/j.chemgeo.2018.11.005>, 2019.
- 455 Yakubovich, O., Podolskaya, M., Vikentyev, I., Fokina, E., and Kotov, A.: U-Th-He Geochronology of Pyrite from the Uzelga VMS Deposit (South Urals)— New Perspectives for Direct Dating of the Ore-Forming Processes, *Minerals*, 10, 1–20, <https://doi.org/10.3390/min10070629>, 2020.

- Yakubovich, O. V., Shukolyukov, Y. a., Kotov, a. B., Brauns, M., Samsonov, a. V., Komarov, a. N., Yakovleva, S. Z.,
460 Sal'nikova, E. B., and Gorokhovskii, B. M.: U-Th-He dating of native gold: First results, problems, and outlooks, *Petrology*,
22, 429–437, <https://doi.org/10.1134/S0869591114050075>, 2014.
- Yakubovich, O. V., Stuart, F. M., Ivanova, E. S., and Gervilla, F.: Constant 4He Concentration and ^{190}Pt - 4He age of Detrital
Pt-Alloy Grains from the Santiago River, Ecuador: Potential as a 4He Mineral Reference Material, *Geostand. Geoanalytical*
Res., 47, 957–968, <https://doi.org/10.1111/ggr.12502>, 2023.
- 465 Yakubovich, O. V, Gedz, A. M., Vikentyev, I. V, Kotov, A. B., and Gorokhovskii, B. M.: Migration of Radiogenic Helium in
the Crystal Structure of Sulfides and Prospects of Their Isotopic Dating, *Petrology*, 27, 59–78,
<https://doi.org/10.1134/S0869591118050089>, 2019.